ACS Partner Journal

CHEM & BIO ENGINEERING

Editors' Choice

Open Access

This article is licensed under CC-BY-NC-ND 4.0

pubs.acs.org/ChemBioEng

Article

Grayscale Color 3D/4D Printing via Orthogonal Photochemistry

Published as part of Chem & Bio Engineering virtual special issue "3D/4D Printing".

Yahui Lu, Chenkai Zhang, Tao Xie,* and Jingjun Wu*

Cite This: *Chem Bio Eng.* 2024, 1, 76–82

Read Online

ACCESS | Metrics & More | Article Recommendations | Supporting Information

ABSTRACT: Coloration is essential for enhancing visual aesthetics and facilitating information communication, but it is difficult to apply to highly complex surfaces. Efficient manufacturing of 3D printed colored products is particularly challenging, given the arbitrary nature of the surfaces. We accomplish this goal with 3D/4D color printing using a photoprintable resin containing a free radical initiator, photocurable monomers, a photoacid generator, and an acid-sensitive dye. The free radical initiator is activated with a long wavelength light (405 nm) for 3D/4D photoprinting. Independently, the photoacid generator is triggered with a shorter wavelength light (365 nm) to activate acid-sensitive dye for coloration. This allows decoupling 3D/4D printing with coloration to yield geometrically complex 3D objects with designable surface color patterns as a highly efficient yet simple way to produce colored 3D objects.

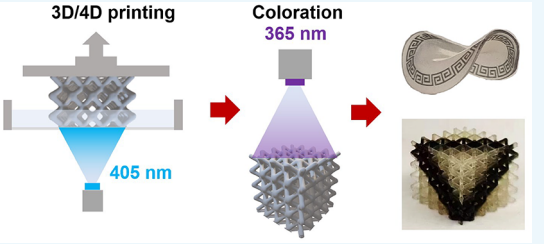

KEYWORDS: *3D/4D printing, coloration, grayscale, orthogonal, photochemistry*

INTRODUCTION

Coloration plays a critical role in the manufacturing industry as a vital link between products and consumers. Conventionally, this is achieved through ink printing on 2D flat substrates, facilitating cost-effective mass production.[1] However, efficient coloration presents limitations when it comes to intricate 3D objects, despite the added product values. Not only does coloration on 3D objects enhance visual aesthetics,[2] but it also serves as a medium for information encryption and communication.[3,4] As an alternative to manual post-painting methods, transferring colored thermoplastic films onto the surface of 3D printed objects is also well established.[5] This method, however, is only applicable to relatively simple 3D topographic surfaces. Coloring more complexed 3D surfaces such as grid and hollow structures as frequently encountered in 3D printing remains challenging.

3D printing is capable of fabricating complex structures without the costly and time-consuming molding-making procedures and has been widely applied in various fields including soft robots,[6,7] medical devices,[8,9] and wearable electronics.[10,11] Decorating 3D printed objects with intricate color patterns is important, but this is mostly realized by manual coloration. Multi-material 3D printing such as PolyJet employs an array of nozzles to eject different materials pixel-by-pixel,[12,13] allowing high freedom for color integration. However, its low printing efficiency and high cost of specialized printers limit its widespread adoption.

Digital Light Processing (DLP) printing offers notable advantages in terms of speed, cost, and simplicity, due to its layer-by-layer printing characteristics.[14,15] However, the use of a single printing precursor in a typical DLP printing setup prohibits the creation of color patterns. Multi-material DLP printing enables direct printing of colored parts using two convertible resin tanks,[16] but the printing efficiency is severely compromised because it requires a complex vat-switching device and cleaning manipulations to avoid cross-contamination.[17] An elegant approach reported by Qi's group employed a special dye in grayscale DLP printing.[18−20] The dye can be oxidized by the free radicals released from the photoinitiators and change the color.[21,22] For this process, however, polymerization kinetics and coloration are both directly coupled to the photoinitiation. Thus, the printed material properties and color are both determined by the intensity of the curing light. This inherent coupling means that independent control of the materials and colors is difficult. In addition, the presence of any residual visible light photoinitiators in the printed material, as is common for DLP printing, may cause unintended color generation unless the products are kept away from daily light.

To address the aforementioned issues, we demonstrate here a 3D color printing method employing orthogonal photochemistry. In our design, the photocurable resin contains a free radical photoinitiator, a photoacid generator, and an acid-sensitive dye. The free radical photoinitiator can be activated with light of 405 nm wavelength for polymerization/printing.

Received: November 8, 2023
Revised: December 22, 2023
Accepted: December 24, 2023
Published: January 4, 2024

ACS Publications

© 2024 The Authors. Co-published by Zhejiang University and American Chemical Society

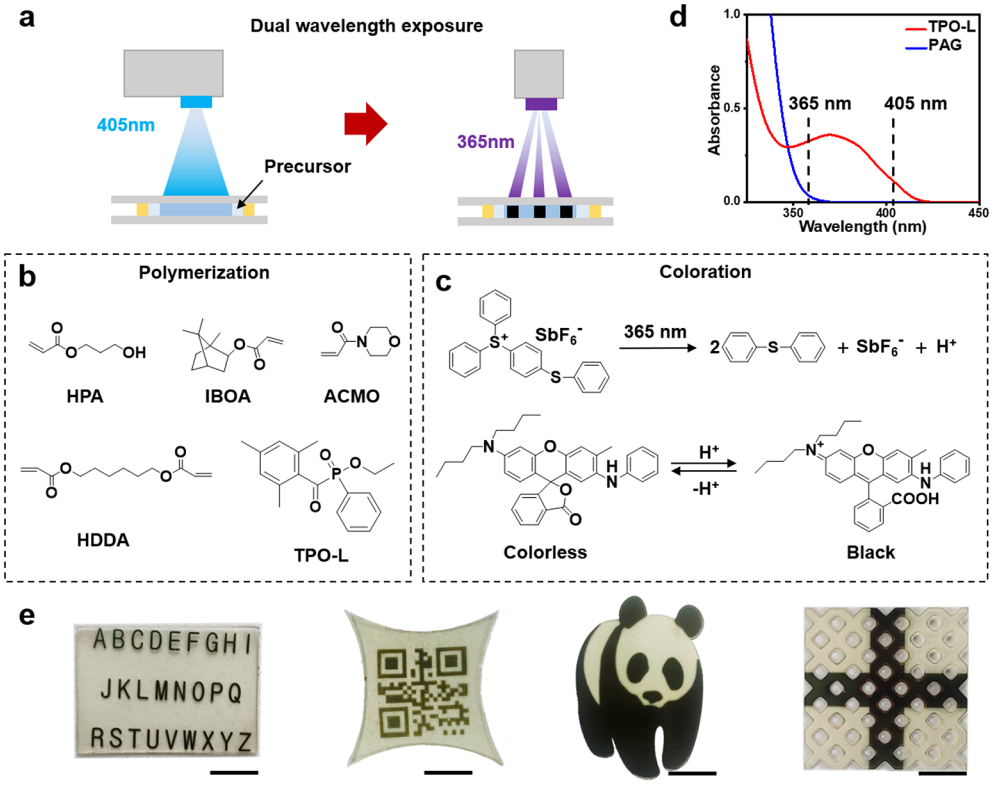

Figure 1. Fabrication of colored 2D films. (a) Schematic illustration of the fabrication process. (b) Chemical structures of polymerization components. (c) Principle of coloration. (d) UV−vis spectra of TPO-L and PAG. (e) Colored 2D films with freely defined shape and color patterns. Thickness: 0.5 mm. Scale bar: 1 cm. The digital printing files for the Panda are from "Panda keychain for single extruder" by Simon Vance, use under CC BY 4.0.[23]

After 3D printing, the photoacid generator is activated under UV light (365 nm) and further reacted with an acid-sensitive dye for coloration. The orthogonal photochemistry allows independent control of the 3D printing and the color generation. As such, 3D objects with complex color patterns can be created by using the simplest DLP printer. In addition, the principle can be extended to 4D printing to create intricate color patterns on topographically complexed surfaces. Our work introduces a highly efficient way for producing 3D objects with color patterns using a single photocurable resin without the need for specific equipment.

RESULTS AND DISCUSSION

For simplicity, we first demonstrate the underlying chemistry principle and specific material design using 2D films. A liquid printing precursor is sandwiched between two glass slides separated by a spacer (Figure 1a). Exposure to light of 405 nm wavelength triggers the free radical polymerization, and subsequent exposure to light of 365 nm wavelength on the cured polymer induces coloration. To enable that, the precursor contains both the polymerization and coloration components. The polymerization components (Figure 1b) include isobornyl acrylate (IBOA), hydroxypropyl acrylate (HPA), 1,6-hexanediol diacrylate (HDDA, fixed at 5%), 4-acryloylmorpholine (ACMO, 5% unless otherwise noted), and a visible-light photoinitiator (TPO-L). Here, the weight ratio between IBOA and HPA is fixed at 7:3. The coloration components (Figure 1c) consist of a photoacid generator (PAG) and an acid-sensitive dye (2-anilino-3-methyl-6-(dibutylamino)fluoran), in which the light activation of the PAG generates protons that change the dye from colorless to black. The wavelength selectivity between TPO-L and PAG is characterized by UV−vis absorbance. As shown in Figure 1d, the cutoff wavelengths of TPO-L and PAG are 420 and 370 nm, respectively. This makes it possible to control the processes of polymerization and coloration independently by using 405 and 365 nm lights. The advantage of the overall design is that not only the shape pattern but also the color patterns can be freely defined through masked light exposures. As shown in Figure 1e, different color patterns can be created on a photocured 2D film with different geometric shapes.

To achieve optimal coloration performance, including contrast and resolution, it is essential to conduct systematic optimization of the resin's composition. The light transmission across the visible wavelength range is investigated for the cured films containing varied weight percentages of the dye and PAG after 365 nm exposure for a fixed time of 60 s. The presence of more dye (Figure 2a) or PAG (Figure 2b) leads to a reduced transparency, implying a darker color. Considering the light transmission and the solubility within the resin, the dye and PAG contents are fixed hereafter at 0.2% and 4%, respectively. Despite the negligible absorption of PAG at 405 nm (Figure 1d), we observe that a reference cured sample containing no ACMO monomer experiences some reduction in transparency (Figure 2c) after extended curing under DLP light (5 mW/cm^2). We believe this is because the light source of the DLP printer is not strictly 405 nm, implying that a small amount of PAG may have been activated in this process. This is why 5% of a functional monomer ACMO is present in our standard precursor. Compared to the dye, the slightly alkaline ACMO

https://doi.org/10.1021/cbe.3c00088
Chem Bio Eng. 2024, 1, 76−82

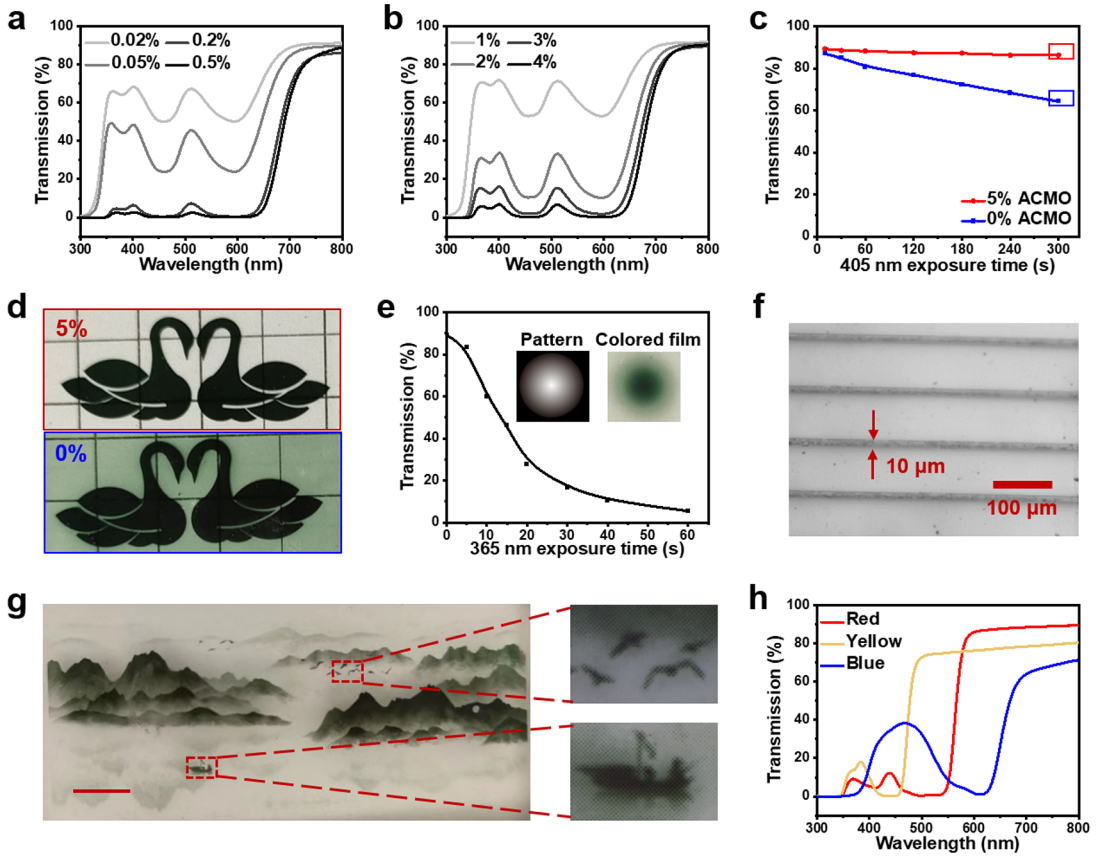

Figure 2. Optimization of the coloration process. (a) Impact of dye content on light transmission, with the PAG content fixed at 0.2%. Thickness: 0.1 mm. (b) The impact of PAG content on light transmission, with the dye content fixed at 4%. (c) Comparison of light transmission of the cured films containing 0 and 5% ACMO, respectively. (d) The photographs of the cured films containing 0 and 5% ACMO, respectively. (e) The dependence of light transmission (600 nm) on light exposure. (f) Photograph of a colored stripe array. (g) A grayscale landscape painting with fine details. Scale bar: 1 cm. (h) Transmission of red, yellow, and blue dye.

has a greater affinity for binding with the protons released by PAG (Figure S1). The incorporation of ACMO not only enhances the color stability (Figure 2c) but also increases the contrast between the colorless and the black regions (Figure 2d). The coloration kinetics was monitored by UV−vis spectra (Figure 2e). Under continuous 365 nm exposure (30 mW/cm^2), the light transmission at 600 nm (the characteristic wavelength) continuously declines to below 15% at 40 s and approaches an even lower value at about 60 s, implying the end of the photoinduced coloration. Utilizing a UV projector (365 nm) as a digital photomask, a patterned stripe array with a feature size of 10 μm can be obtained (Figure 2f). It is possible to reduce the feature size further with a higher resolution projector. Here, the advantage of using a digital UV projector is the ability to provide grayscale exposure. This means that through a single exposure, different regions can accurately receive varying levels of light energy, resulting in patterns with different transparencies or grayscale values. Based on this principle, a grayscale landscape painting with fine details is created (Figure 2g). Besides black, other acid-sensitive dyes (supporting information) may also be selected to create different colors including red, yellow, and blue (Figure 2h and Figure S2). Mixing these dyes in different proportions will obtain a wider color palette for 3D printed objects (Figure S3).

The aforementioned resins can be readily 3D printed with a DLP printer equipped with a 405 nm wavelength light source. After the 3D printing, color patterns on selective areas can be generated with 365 nm light exposure (Figure 3a). For the 3D printing, the photocuring kinetics were investigated by FTIR spectra (Figure S4). The double bond conversion reached a maximum plateau value of 90% after 25 s (Figure 3b). The material shows no obvious color change at this time scale. In principle, one can integrate both the 405 and 365 nm light sources directly into the 3D printer, which would enable us to alternately utilize these two light sources for controlling material curing and coloration. This would allow us to achieve one-step 3D printing of grayscale colored 3D objects. In reality, we do not have the hardware to demonstrate this at this stage although this is an interesting direction to go in the future. For the current study, we continue to rely on the post-printing light exposure process (365 nm) for coloration to illustrate the principle. For selective coloration, the intended non-colored regions are physically masked. With this approach, a series of 3D printed objects with color patterns are successfully created (Figure 3c). Notably, the mechanical properties of the material are not affected by 365 nm exposure (Figures S5 and S6). For certain 3D shapes, such as large-curvature shapes and multilayer structures (Figure 3d), access to light for coloration is difficult. One interesting way to overcome this issue is to make use of the shape memory behavior of the printed material. Its shape memory cycles confirm its robust shape memory behavior with shape fixity and shape recovery ratios, both above 95% (Figure S7). As demonstrated in Figure 3d, with shape memory capability, the

https://doi.org/10.1021/cbe.3c00088
Chem Bio Eng. 2024, 1, 76−82

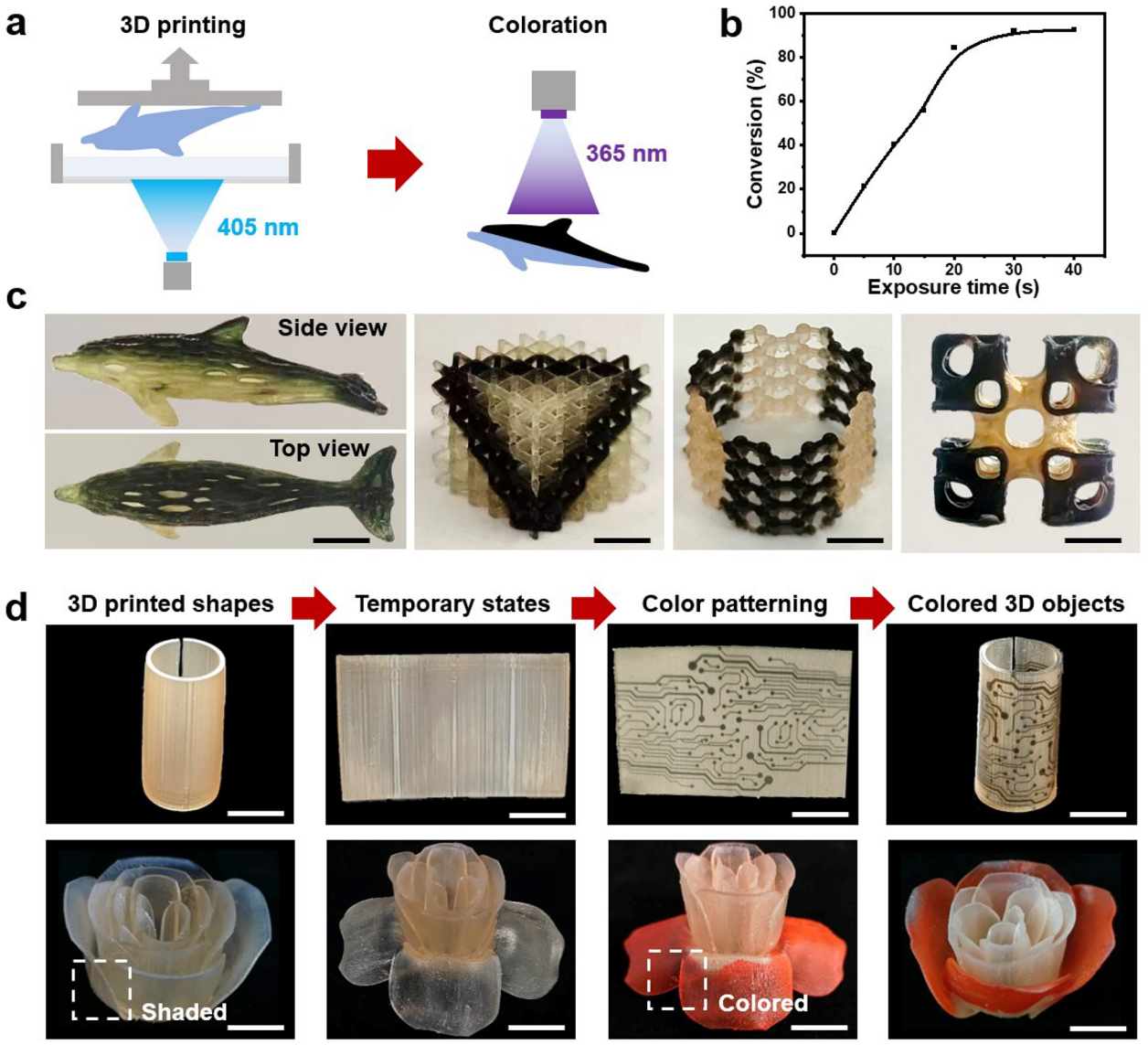

Figure 3. 3D color printing. (a) Schematic illustration of the colored 3D printing. (b) Curing kinetics under 405 nm DLP light. (c) 3D color printed parts (scale bar: 1 cm.) The 3D printing files: the first is from "Voronoi Dolphin" by TK3DPrinting, use under CC BY 4.0.[23] The third is from "Carbon Nanotube" by otache, use under CC BY-SA 3.0.[23] The forth is from "Cubic Lattice" by O3D, use under CC BY 4.0.[23] (d) 4D color printing using shape memory effect. (Scale bar: 1 cm.) The second series is from "Rose with stem" by tc_fea, use under CC BY 4.0.[23]

printed material in 3D shapes can be deformed into temporary flattened states, which allows light exposure for color patterning. After that, the flattened temporary shapes are recovered upon heating to their original 3D shapes. This overall process allows efficient color integration on geometrically complexed parts.

A more direct way of coloration of 3D surface contours without having to utilize the shape memory effect is by direct 4D printing. Previous studies have demonstrated that 4D printing allows for the fabrication of complex 3D shapes by introducing heterogeneity into 2D photocured films.[24,25] Upon releasing the internal stress (e.g., via removal of unreacted monomers), the heterogeneity allows transformation of a 2D film into a 3D object. We deduce that in such a process color patterns can be generated at the 2D state, which would eventually be converted into a 3D colored object. This is schematically illustrated in Figure 4a. A first light pattern (405 nm) defines the heterogeneous photocuring that determines the 3D shape, whereas a second light pattern (365 nm) generates the color pattern. Specifically, for the current system, the liquid precursor is cured by 405 nm light, with spatiotemporal control of both the light exposed locations and the exposure time. The exposure time affects the degree of curing and consequently mass loss due to unreacted monomer removal after curing. Overall, this leads to reduction of mass loss with longer light exposure time (Figure 4b). Importantly, the film is designed to be optically thick enough to create a gradient in curing in the thickness direction,[23] consequently generating asymmetry. Thus, upon monomer removal, the cured film is transformed into a curved geometry, with the curvature reduced with the exposure time (Figure 4c). This principle, coupled with controlling the light exposed area, allows access to 4D printed geometries.

In the examples shown in Figure 3, the exposure to 365 nm light only introduces color but does not affect the geometry of the printed parts. For the direct 4D printing process in Figure

https://doi.org/10.1021/cbe.3c00088
Chem Bio Eng. 2024, 1, 76−82

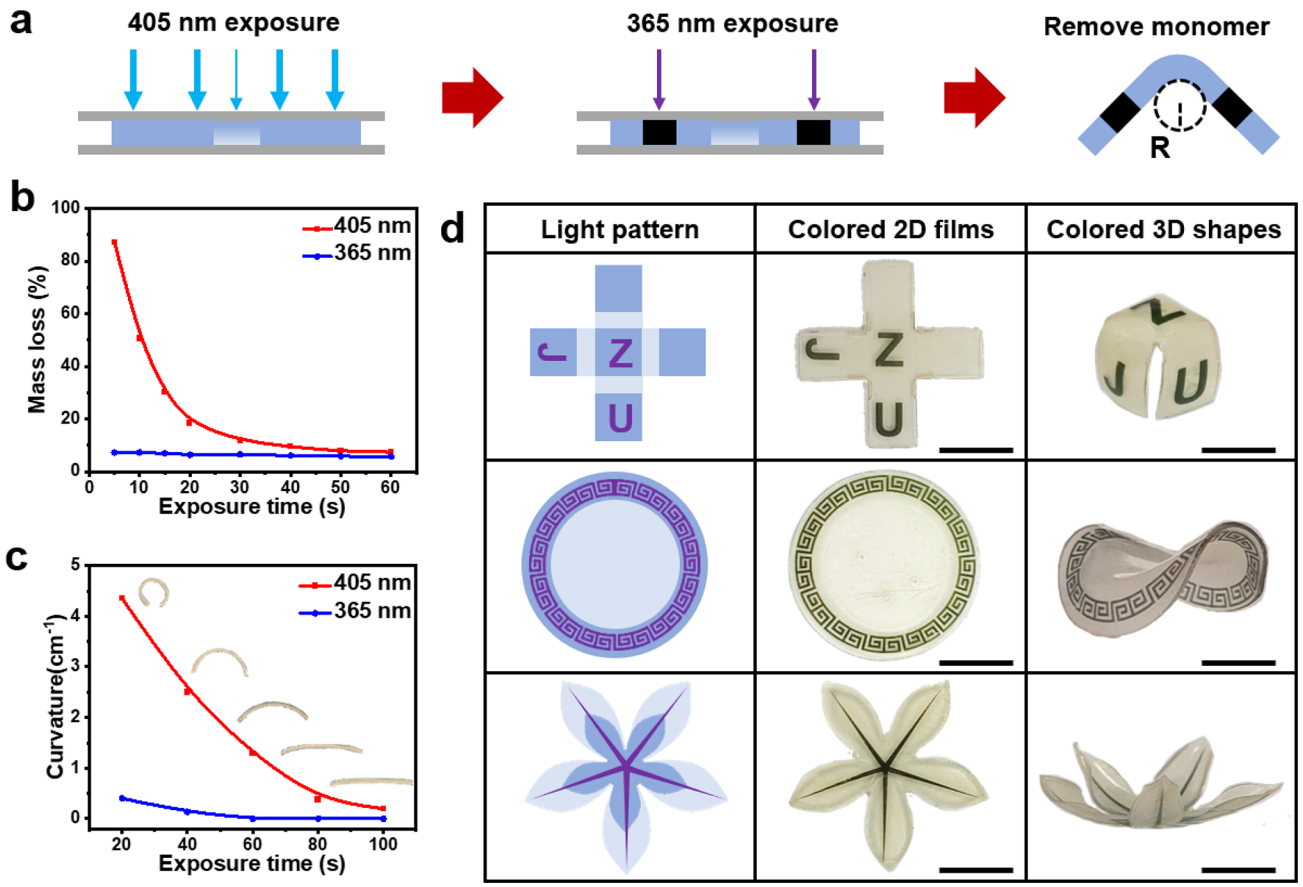

Figure 4. Coloration by 4D printing processing. (a) Schematic illustration of 4D color printing. (b) Impact of light exposure on the mass loss. (c) Impact of light exposure on the curvature created after unreacted monomer removal. (d) 4D color printed parts with color patterns. In the light patterns, the light and dark blue regions denote 405 nm light exposure times of 20 and 80 s, respectively. The purple regions in the light pattern denote 365 nm light exposure time of 40 s. Thickness: 0.5 mm. Scale bar: 1 cm.

4a, however, the precursor may be far from full curing. Further exposure to 365 nm light would trigger its rapid curing, as implied by the low mass loss corresponding to the blue curve in Figure 4b. This would negatively interfere with the subsequent 4D shape transformation, as the significant reduction of curvature (blue curve in Figure 4c) indicates. To address this issue, we focus on generating colors (365 nm exposure) in regions where the 405 nm exposure time is 80 s, which is sufficiently long to avoid a negative impact. With this process, a light pattern consisting of two distinct light patterns (405 and 365 nm, respectively) is turned into a colored 2D film, which transforms further into a 3D colored object including the cube, saddle, and flower shown in Figure 4d.

CONCLUSION

In summary, we report a simple yet versatile approach to fabricating colored 3D objects. The underlying principle is to utilize orthogonal photochemistries (405 and 365 nm lights) with one defining the 3D shape and the other determining the color patterns. The formulated photoresin is compatible with well-established DLP 3D printing and 4D printing technologies, offering diverse options for coloring 3D objects based on their unique characteristics. These options include post-printing coloration directly on 3D printed objects, post-printing coloration on temporary shapes defined with the shape memory effect, and coloration during direct 4D photoprinting. In the future, we aim to integrate the coloration principles with dual light sources built into the printing hardware and expand the grayscale coloring into multiple coloring. In addition, it is possible to extend the underlying orthogonal photochemistry to introduce other material functions beyond colors.

EXPERIMENTAL SECTION

Materials. Isobornyl acrylate (IBOA), hydroxypropyl acrylate (HPA), 1,6-hexanediol diacrylate (HDDA), and 4-acryloylmorpholine (ACMO) were all purchased from Macklin. The photoinitiator (TPO-L) and photoacid generator (PAG 6976) were procured from Guangzhou Lihou Trading Corporation. The acid-sensitive dyes were bought from Shanghai Yuanye Bio-Technology Co. Ltd. All chemicals were used as received.

Precursor and Curing of 2D Films. In a typical experiment, IBOA (70 g), HPA (30 g), HDDA (5 g), ACMO (5 g), PAG (4 g), TPO-L (2 g), and the acid-sensitive dye (0.2 g) were fully mixed at 80 °C. The precursor solution was injected into a mold consisting of two pieces of quartz glass separated with a silicon rubber spacer. The projector from a bottom-up 3D printer (Shining 3D, AccuFab-D1s) was employed to provide 405 nm exposure for curing.

3D Printing. The parts were printed by a bottom-up 3D printer (Shining 3D, AccuFab-D1s). All of the printing models were printed using a slice thickness of 100 μm. The exposure time was 30 s for each layer. The printed parts were post-cured in a visible light chamber (20 mW/cm^2, 405 nm).

Coloration. The UV light source (365 nm) was obtained from Shenzhen Taoyuan Optoelectronics Co., Ltd. (intensity: 30 mW/cm^2).

https://doi.org/10.1021/cbe.3c00088
Chem Bio Eng. 2024, 1, 76−82

Color 4D Printing. The precursor was injected into a mold. It was photocured with masked 405 nm light. It was subsequently exposed to 365 nm light. Afterward, it was put in a thermal oven (120 °C) to remove the unreacted monomers to yield the 3D shapes.

Characterization. For curing kinetics, the double bond conversions were measured by a real-time FTIR spectrometer (Thermo Fisher Scientific, Nicolet, 5700). The intensity ratio ($A_{vinyl}/A_{carbonyl}$) was calculated as the ratio between the peak area of vinyl group (810 cm^{-1}) and that of carbonyl group (1720 cm^{-1}). The double bond conversion was calculated as $\alpha_{vinyl,t} = 1 - (A_{vinyl}/A_{carbonyl})_t/(A_{vinyl}/A_{carbonyl}))_{t=0}$, where t is the exposure time. The absorbance of the photoinitiator and light transmission of the cured films (thickness: 0.1 mm) were measured using a UV−vis spectrophotometer (Shimadzu UV-2600, Japan). The printing resolution was determined with an optical microscope (Zeiss, ZCEC-150348F). The differential scanning calorimetry (DSC) measurement was conducted with a TA Q200 instrument at a heating rate of 5 °C/min. The shape memory properties of the materials were quantitatively evaluated by using a dynamic mechanical analyzer (DMA, TA Q800).

■ ASSOCIATED CONTENT

Data Availability Statement

The data that support the findings of this study are available from the corresponding author upon reasonable request.

Supporting Information

The Supporting Information is available free of charge at https://pubs.acs.org/doi/10.1021/cbe.3c00088.

The effect of the addition of ACMO, four typical acid-sensitive dyes, photograph of coloration, FTIR spectra, DSC curves, strain−stress curves, quantitative shape memory cycles of the samples (PDF)

■ AUTHOR INFORMATION

Corresponding Authors

Tao Xie − *State Key Laboratory of Chemical Engineering, College of Chemical and Biological Engineering, Zhejiang University, Hangzhou 310027, China;* orcid.org/0000-0003-0222-9717; Email: taoxie@zju.edu.cn

Jingjun Wu − *State Key Laboratory of Chemical Engineering, College of Chemical and Biological Engineering, Zhejiang University, Hangzhou 310027, China; Ningbo Innovation Center, Zhejiang University, Ningbo 315807, China;* orcid.org/0000-0002-9026-5541; Email: jingjunwu@zju.edu.cn

Authors

Yahui Lu − *State Key Laboratory of Chemical Engineering, College of Chemical and Biological Engineering, Zhejiang University, Hangzhou 310027, China*

Chenkai Zhang − *State Key Laboratory of Chemical Engineering, College of Chemical and Biological Engineering, Zhejiang University, Hangzhou 310027, China*

Complete contact information is available at: https://pubs.acs.org/10.1021/cbe.3c00088

Notes

The authors declare no competing financial interest.

■ ACKNOWLEDGMENTS

This work was supported by the National Natural Science Foundation (No. 22375176) and the National Key R&D Program of China (No. 2022YFB3805701).

■ REFERENCES

(1) Xi, G.; Sheng, L.; Du, J.; Zhang, J.; Li, M.; Wang, H.; Ma, Y.; Zhang, X. Water assisted biomimetic synergistic process and its application in water-jet rewritable paper. *Nat. Commun.* **2018**, *9*, 4819.

(2) Zhang, Y.; Zhang, L.; Zhang, C.; Wang, J.; Liu, J.; Ye, C.; Dong, Z.; Wu, L.; Song, Y. Continuous resin refilling and hydrogen bond synergistically assisted 3D structural color printing. *Nat. Commun.* **2022**, *13*, 7095.

(3) Zhang, Y.; Le, X.; Jian, Y.; Lu, W.; Zhang, J.; Chen, T. 3D Fluorescent hydrogel origami for multistage data security protection. *Adv. Funct. Mater.* **2019**, *29*, No. 1905514.

(4) Chen, D.; Ni, C.; Yang, C.; Li, Y.; Wen, X.; Frank, C.; Xie, T.; Ren, H.; Zhao, Q. Orthogonal photochemistry toward direct encryption of a 3D-printed hydrogel. *Adv. Mater.* **2023**, *35*, No. 2209956.

(5) Zhang, Y.; Tong, Y.; Zhou, K. Coloring 3D printed surfaces by thermoforming. *IEEE Transactions on Visualization & Computer Graphics* **2017**, *23*, 1924−1935.

(6) Xing, R.; Yang, J.; Zhang, D.; Gong, W.; Neumann, T.; Wang, M.; Huang, R.; Kong, J.; Qi, W.; Dickey, M. Metallic gels for conductive 3D and 4D printing. *Matter* **2023**, *6*, 2248−2262.

(7) Peng, X.; Wu, S.; Sun, X.; Yue, L.; Montgomery, M.; Demoly, F.; Zhou, K.; Zhao, R.; Qi, H. 4D printing of freestanding liquid crystal elastomers via hybrid additive manufacturing. *Adv. Mater.* **2022**, *34*, No. 2204890.

(8) Zhou, T.; Yuk, H.; Hu, F.; Wu, J.; Tian, F.; Roh, H.; Shen, Z.; Gu, G.; Xu, J.; Lu, B.; Zhao, X. 3D printable high-performance conducting polymer hydrogel for all-hydrogel bioelectronic interfaces. *Nat. Mater.* **2023**, *22*, 895−902.

(9) Ge, Q.; Chen, Z.; Cheng, J.; Zhang, B.; Zhang, Y.; Li, H.; He, X.; Yuan, C.; Liu, J.; Magdassi, S.; Qu, S. 3D printing of highly stretchable hydrogel with diverse UV curable polymers. *Sci. Adv.* **2021**, *7*, No. eaba4261.

(10) Hensleigh, R.; Cui, H.; Xu, Z.; Massman, J.; Yao, D.; Berrigan, J.; Zheng, X. Charge-programmed three-dimensional printing for multi-material electronic devices. *Nat. Electron.* **2020**, *3*, 216−224.

(11) Chen, J.; Zhao, L.; Zhou, K. Multi-Jet fusion 3D voxel printing of conductive elastomers. *Adv. Mater.* **2022**, *34*, No. 2205909.

(12) https://www.materialise.com/en/industrial/3d-printing-technologies/polyjet.

(13) Larson, N.; Muller, J.; Chortos, A.; Davidson, Z.; Clarke, D.; Lewis, J. Rotational multimaterial printing of filaments with subvoxel control. *Nature* **2023**, *613*, 682−688.

(14) Wu, J.; Guo, J.; Linghu, C.; Lu, Y.; Song, J.; Xie, T.; Zhao, Q. Rapid digital light 3D printing enabled by a soft and deformable hydrogel separation interface. *Nat. Commun.* **2021**, *12*, 6070.

(15) Deng, S.; Wu, J.; Dickey, M.; Zhao, Q.; Xie, T. Rapid open-air digital light 3D printing of thermoplastic polymer. *Adv. Mater.* **2019**, *31*, No. 1903970.

(16) Chen, L.; Zhang, Y.; Ye, H.; Duan, G.; Duan, H.; Ge, Q.; Wang, Z. Color-changeable four-dimensional printing enabled with ultraviolet-curable and thermochromic shape memory polymers. *ACS Appl. Mater. Interfaces* **2021**, *13*, 18120−18127.

(17) Cheng, J.; Wang, R.; Sun, Z.; Liu, Q.; He, X.; Li, H.; Ye, H.; Yang, X.; Wei, X.; Li, Z.; Jian, B.; Deng, W.; Ge, Q. Centrifugal multimaterial 3D printing of multifunctional heterogeneous objects. *Nat. Commun.* **2022**, *13*, 7931.

(18) Kuang, X.; Wu, J.; Chen, K.; Zhao, Z.; Ding, Z.; Hu, F.; Fang, D.; Qi, H. Grayscale digital light processing 3D printing for highly functionally graded materials. *Sci. Adv.* **2019**, *5*, No. eaav5790.

(19) Yue, L.; Montgomery, S.; Sun, X.; Yu, L.; Song, Y.; Nomura, T.; Tanaka, M.; Qi, H. Single-vat single-cure grayscale digital light processing 3D printing of materials with large property difference and high stretchability. *Nat. Commun.* **2023**, *14*, 1251.

(20) Yue, L.; Sun, X.; Yu, L.; Li, M.; Montgomery, S.; Song, Y.; Nomura, T.; Tanaka, M.; Qi, H. Cold-programmed shape-morphing structures based on grayscale digital light processing 4D printing. *Nat. Commun.* **2023**, *14*, 5519.

(21) Peng, R.; Yue, L.; Liang, S.; Montgmery, S.; Lu, C.; Cheng, C.; Beyah, R.; Zhao, R.; Qi, H. Multi-color 3D printing via single-vat grayscale digital light processing. *Adv. Funct. Mater.* **2022**, *32*, No. 2112329.
(22) Zhu, G.; Liu, M.; Weng, S.; Zhang, G.; Hu, Y.; Kou, Z.; Bo, C.; Hu, L.; Wu, S.; Zhou, Y. Dye-free and reprintable multi-color DLP 3D printing using $ZnCl_2$-based polymerizable deep eutectic solvents and type I photoinitiators. *Chem. Eng. J.* **2023**, *472*, No. 144987.
(23) UltiMaker Thingiverse. https://www.thingiverse.com/ (accessed 2023-7-10).
(24) Zhang, Y.; Huang, L.; Song, H.; Ni, C.; Wu, J.; Zhao, Q.; Xie, T. 4D printing of a digital shape memory polymer with tunable high performance. *ACS Appl. Mater. Interfaces* **2019**, *11*, 32408−32413.
(25) Fang, M.; Liu, T.; Xu, Y.; Jin, B.; Zheng, N.; Zhang, Y.; Zhao, Q.; Jia, Z.; Xie, T. Ultrafast digital fabrication of designable architectured liquid crystalline elastomer. *Adv. Mater.* **2021**, *33*, No. 2105597.

https://doi.org/10.1021/cbe.3c00088
Chem Bio Eng. 2024, 1, 76−82